

Single-Molecule Magnet Behavior with a Single Metal Center Enhanced through Peripheral Ligand Modifications

Titel Jurca, Ahmed Farghal, Po-Heng Lin, Ilia Korobkov, Muralee Murugesu,* and Darrin S. Richeson*

Centre for Catalysis Research and Innovation and Department of Chemistry, University of Ottawa, Ottawa, Ontario, K1N 6N5, Canada

S Supporting Information

ABSTRACT: Bis(imino)pyridine pincer ligands in conjunction with two isothiocyanate ligands have been used to prepare two mononuclear Co(II) complexes. Both complexes have a distorted square-pyramidal geometry with the Co(II) centers lying above the basal plane. This leads to significant spin–orbit coupling for the d^7 Co(II) ions and consequently to slow relaxation of the magnetization that is characteristic of Single-Molecule Magnet (SMM) behavior.

Single-Molecule Magnets, SMMs, arise when discrete molecular species retain a magnetic moment after removing an applied magnetic field. The associated barrier to magnetic relaxation originates from the action of negative molecular uniaxial magnetic anisotropy (D) on a nonzero spin ground state (S), producing the barrier given by the expression $U = S^2|D|$ for integer and $(S^2 - 1/4)|D|$ for half integer spins. First discovered more than a decade ago, SMMs were initially limited to transition metal clusters.¹ Recently, molecules containing a single paramagnetic lanthanide or actinide metal center have been shown to exhibit slow magnetic relaxation at low temperature.² Current reports from Chang, Long and co-workers demonstrate that SMM behavior is possible for mononuclear Fe(II) complexes.^{3,4} In these monometallic SMMs, the highly anisotropic ground state is generated by strong spin–orbit coupling. In the case of the Fe(II) compounds, these air-sensitive species were designed around a unique, rigid ligand scaffold that enforced a 3-fold coordination geometry and maintained a ground state with unquenched orbital angular momentum and a high-spin $S = 2$ value. Our objective is to exploit the inherent magnetic anisotropy of a high-spin cobalt(II) center ($S = 3/2$), enhanced by controlling the metal coordination environment through simple substituent modification of a well-known ligand array, to induce formation of air-stable Single-Molecule Magnets possessing a single cobalt center. We now report the observation of slow magnetic relaxation for this species.

The neutral, planar bis(imino)pyridine pincer ligands, $2,6\text{-}\{\text{ArN}=\text{C}(\text{R})\}_2\text{NC}_5\text{H}_3$, pioneered for their ability to stabilize Co and Fe polymerization catalysts,⁵ have lately been elegantly exploited to stabilize low valent cobalt complexes and allow their engagement in innovative transformations.⁶ Our attraction to the bis(imino)pyridine scaffolds was initiated by the goal of employing these species for preparing unprecedented structure and bonding arrangements with low valent main group metal complexes.⁷ This has expanded into the fine-tuning of metal binding geometry through variation of the R and Ar groups, using the modular and direct synthetic routes to these ligands. In particular, we anticipated the rigid base provided by these ligands

could be exploited to favor a square pyramidal over a trigonal bipyramidal coordination geometry and, in turn, induce a larger zero-field splitting D parameter.⁸ We further targeted the introduction of phenyl substituents in the imine positions ($\text{R} = \text{Ph}$, **2**) anticipating that this would impact the geometry of the coordinated metal center to induce a distorted geometry and compel the Co(II) center to move out of the basal plane. Finally, in an effort to enhance the structural modulation of the magnetic features we chose to employ ambidentate isothiocyanate ligands that occupy a single coordination site and thus will accommodate flexibility in metal geometry.

The direct reaction of $\text{Co}(\text{NCS})_2$ with ligands **1** and **2** (Scheme 1) proceeded in nearly quantitative yield to generate paramagnetic, green **3** ($[\{\text{ArN}=\text{CMe}\}_2(\text{NPh})]\text{Co}(\text{NCS})_2$, 97%) and brown-green **4** ($[\{\text{ArN}=\text{CPh}\}_2(\text{NPh})]\text{Co}(\text{NCS})_2$, 95%), respectively.⁹ UV–vis spectra of these two compounds revealed very similar profiles with **4** displaying a slightly blue-shifted (≤ 8 nm) spectrum (Figure S1). The room temperature magnetic susceptibilities of **3** and **4** (1000 Oe) afforded χT values of 3.01 and $3.05 \text{ cm}^3 \text{ K/mol}$, respectively. These values, while larger than the anticipated spin-only value for $S = 3/2$ of $1.87 \text{ cm}^3 \text{ K/mol}$, are well within the range of $2.1\text{--}3.4 \text{ cm}^3 \text{ K/mol}$ for experimentally observed highly anisotropic Co^{II} ions.¹⁰ These observations suggested significant spin–orbital coupling in these d^7 complexes and encouraged a structural examination by single crystal X-ray analysis.

The results of structural analyses for **3** and **4** are presented in Figure 1. As anticipated, the pentacoordinate Co(II) centers reside in distorted square pyramidal geometries in which the coordinated nitrogen atoms from the chelate ligand and from one isothiocyanate form the base. The coordination sphere is completed by a second isothiocyanate ligand in the apical position.¹¹ The diisopropylaryl substituents on the coordinated imine nitrogen centers are essentially orthogonal to the basal plane of the complex. In the case of compound **4**, the phenyl substituents of the iminocarbon atoms are clearly rotated out of the plane of the Schiff base functional groups, to avoid steric interaction with the bulky Ar substituents and contact with the central pyridyl group. The role of the ligand R groups on distortion of the metal geometry is also revealed by these structures. In **3**, the cobalt sits above the basal N_4 mean plane by 0.39 \AA . Changing the substituent to $\text{R} = \text{Ph}$ (**4**) leads to a more pronounced distortion with a metal center lying out of the basal N_4 plane by 0.52 \AA .

While there are no short intermolecular contacts in the structures of either of these species, compound **4** does display

Received: May 18, 2011

Published: September 07, 2011

Scheme 1

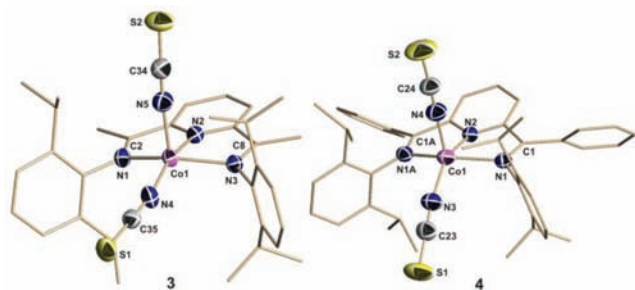
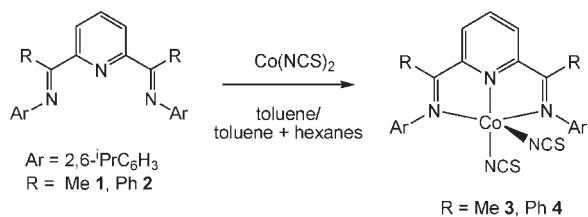
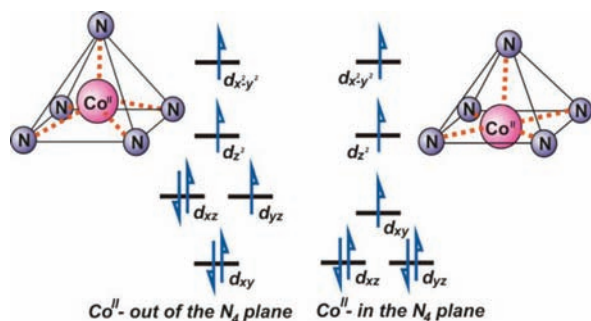


Figure 1. Structure and selected atom numbering scheme of compounds 3 (left) and 4 (right). Hydrogen atoms and cocrystallized solvents omitted for clarity.

Scheme 2. Simplified Model of d-Orbital Energy Diagram for a Square-Based Pyramid with the Metal out of the Basal Plane (Left) and in the Basal Plane (Right)



an interesting packing arrangement. Specifically, the S2 center of the apical isothiocyanate is oriented toward the open face of an adjacent Co center along the *c*-axis (*d* = 5.06 Å). However, the Co centers remain separated by 8.67 Å (see Figure S2). The methyl analogue, 3, does not display any such long distance interaction, and the shortest Co–Co distance in the structure of 3 is 9.90 Å.

The elevation of the Co centers out of the square pyramidal basal plane, as is observed for compounds 3 and 4, has a profound effect on spin–orbit coupling for these species. A simplified model for the orbital configuration that is associated with this distortion is shown in Scheme 2 and reveals the significant spin–orbit coupling arising from the 90° rotational transformation along the *z*-axis between the partially filled degenerate *d*_{*xy*}, *d*_{*yz*} orbitals.¹² In contrast, an ideal square pyramidal coordination geometry with the metal center lying in the basal plane displays lower lying, degenerate *d*_{*xy*}, *d*_{*yz*} orbitals that are fully occupied.

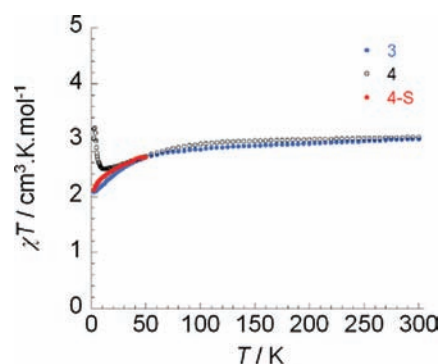


Figure 2. Temperature dependence of the χT product at 1000 Oe for complexes 3 and 4 (with χ being the molar susceptibility per mononuclear complex defined as M/H). Blue and black data points are for solid samples of 3 and 4, respectively. Red data points (labeled 4-S) are for a THF solution sample of 4.

The combined intrinsic magnetic anisotropy for both complexes with a distorted pentacoordinate environment suggested the likelihood of a very pronounced magnetic anisotropy, and we undertook a comprehensive magnetic study of these compounds. Initially, field dependent magnetization data were collected at 100 K for both complexes, and perfectly linear behavior, which extrapolates to $M = 0$ at 0 Oe, was observed, as expected for samples without any significant ferromagnetic impurities (Figure S3). Subsequently, variable temperature dc susceptibility measurements were collected on powdered crystalline samples of 3 and 4 at a field of 1000 Oe over the 2–300 K temperature range as shown in Figure 2. For both compounds, the χT value remains roughly constant from room temperature to 100 K, before decreasing slightly. This temperature profile is consistent with Curie-type behavior for noninteracting mononuclear Co(II) centers, whereas the observed decrease seen below 100 K is most likely due to intrinsic magnetic anisotropy of the Co(II) ions rather than antiferromagnetic interactions between the spin carriers. For 3, below 100 K the χT product decreases with decreasing temperature to reach a value of 2.07 cm³ K/mol at 2.5 K. In the case of complex 4, the χT value decreases to 2.48 cm³ K/mol at 12 K and then increases rapidly to reach a maximum of 3.21 at 3 K followed by a rapid drop to 3.03 cm³ K/mol at 2.5 K. The sharp increase observed in the latter case is most likely due to intermolecular ferromagnetic interactions, which is a remarkable feature for a mononuclear system with metal centers relatively well separated (8.67 Å). This long-range pathway is likely provided by the apical isothiocyanate oriented toward the open face of an adjacent Co center along the *c*-axis (Figure S2). Such intermolecular interactions can be removed by separating the magnetic centers through solution susceptibility measurements. Therefore, crystals of 4 were fully dissolved in THF in a sealed tube and dc susceptibility measurements were carried out on the resulting frozen solution below 50 K (Figure 2, red dots). As expected, these data parallel the solid-state data showing a clear decrease in χT with decreasing temperature to reach a value of 2.1 cm³ K/mol at 2.5 K. The absence of an increase in χT for this solution sample clearly demonstrates the presence of long-range interactions between the highly anisotropic spin carriers in the solid state of 4. The observation of χT values of 3.01 (for 3) and 3.05 cm³ K/mol (for 4) at room temperature is consistent with the possible value of 3.38 cm³ K/mol ($\mu_{\text{eff}} = [g^2S(S+1) + L(L+1)]^{1/2}$), which includes the orbital contribution.¹⁰

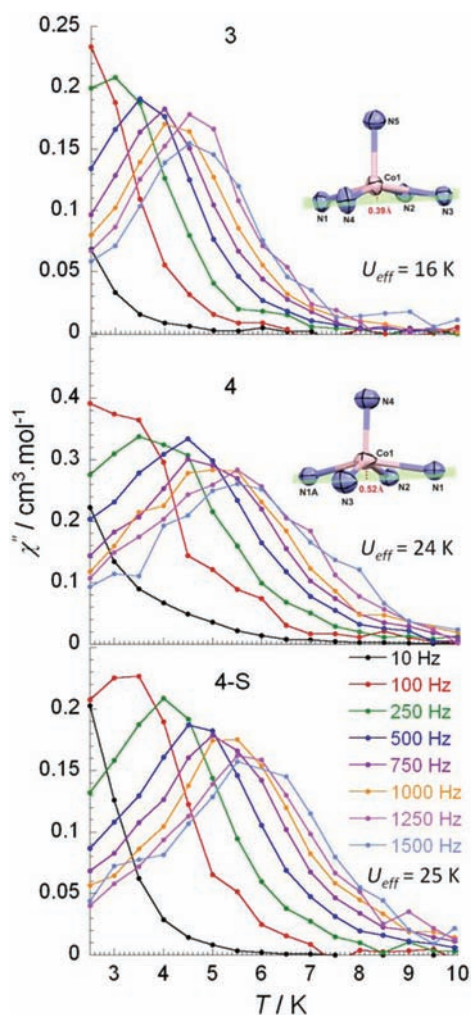


Figure 3. Variable-frequency out-of-phase ac susceptibility data for 3 (top) and 4 (middle: solid state, bottom: solution), collected over the temperature range 2–10 K at under an applied dc field of 2000 Oe. Inset diagrams of the CoN_5 core emphasize the displacement of the metal out of the basal plane at the indicated distances.

The field dependence of the magnetization of 3, 4, and 4-S were performed at fields ranging from 0 to 7 T between 2.2 and 8 K (Figures S4–S9). The M vs H data below 8 K revealed a rapid increase of the magnetization at low magnetic fields. At higher fields, M increases linearly without clear saturation to ultimately reach $3.04 \mu_B$ ($H = 7$ T, at 2.5 K) for 3, $3.2 \mu_B$ ($H = 7$ T, at 2.2 K) for 4, and $2.5 \mu_B$ ($H = 7$ T, at 2.5 K) for 4-S. The lack of saturation and nonsuperposition on a single master curve of M vs H/T data for both complexes also suggests the presence of magnetic anisotropy (Figures S7–S9). Several attempts to fit the reduced magnetization data using the Magnet¹³ program were unsuccessful. The latter program employs matrix diagonalization to a model that assumes only the ground state is populated, includes axial zero-field splitting (DS_z^2) and Zeeman interactions, and incorporates a full powder average. However no rhombic (E) term can be introduced, thus more sophisticated software needs to be employed to achieve reasonable fits. Furthermore, the susceptibility data can be fitted (Figure S10) assuming a simple zero-field splitting effect¹⁴ which leads to D values of -40.5 K for 3 and -40.6 K for 4, imply a significant uniaxial anisotropy.

In order to probe the SMM behavior in complexes 3 and 4, temperature and frequency dependence of the ac susceptibility measurements were measured in the temperature range 2–10 K. These measurements were carried out on a solid state sample for 3 and both solid state and solution phase samples of 4. Under a zero dc field and a 3 Oe ac field oscillating at frequencies between 1 and 1500 Hz, no ac signal was observed. However, when a static dc field was applied, both compounds displayed a frequency dependent signal (Figures 3, S11). Such behavior generally indicates that slow relaxation of the magnetization is subjected to quantum tunneling of the magnetization (QTM) through the spin reversal barrier via degenerate $\pm Ms$ energy levels.³ For an Ising-like anisotropic system, assuming only the lowest energy levels are populated, spins then reverse by QTM via the ground state doublet $\pm S$.¹⁵ It is noteworthy that for a half integer spin system such as 3, or 4, QTM should be suppressed at zero field due to spin parity effects.¹⁶ Therefore, the observed QTM is most likely due to effects such as environmental degrees of freedom as well as hyperfine and dipolar coupling via a transverse field component. Hence, ac measurements under various dc fields were performed in order to determine the optimum field for which the QTM effect would be reduced. This search indicated minima with optimum fields of 700 and 2000 Oe for 3 and 4, respectively (Figure S12). Ac measurements under these optimal applied dc fields reveal a frequency dependent signal with a clear out-of-phase (χ'') peak for both complexes. In order to compare the energy barriers for both complexes ac measurements were carried out under 2000 Oe for solid (3, 4) and solution (4) samples and are shown in Figure 3 (see Figure S11). The observed single relaxation process behavior is indicative of super paramagnet-like slow magnetization relaxation of an SMM.

The anisotropic energy barrier, U_{eff} , can be obtained from the high temperature regime of the relaxation where it is thermally induced (Arrhenius law, $\tau = \tau_0 \exp(U_{\text{eff}}/kT)$). In fact, at a high temperature limit (above 4 K) the data exhibit a linear correlation indicating that it follows the Arrhenius Law. Relaxation times, τ , are extracted from these data allowing the calculation of a thermally induced anisotropic energy barrier, U_{eff} , between the magnetic ground states. The effective energy barriers obtained from the fitting procedure (Figures S13–S14) are $U_{\text{eff}} = 16$ K ($\tau_0 = 3.6 \times 10^{-6}$ s) for 3 and 24 K ($\tau_0 = 5.1 \times 10^{-7}$ s) for 4. The latter U_{eff} of 4 obtained from solid-state measurement was also confirmed through ac measurement on a frozen solution with an effective barrier of 25 K ($\tau_0 = 1.6 \times 10^{-6}$ s) (Figure 3 bottom). This clearly confirms that the slow relaxation of the magnetization is molecular in origin. The observed relaxation mechanism follows thermally activated behavior at high temperature which indicates the Orbach process is the predominant relaxation pathway.¹⁷ Relaxation associated with the thermally activated regime takes place by excitation to higher $M_s = \pm 1/2$ level with the absorption of phonons from the lattice, followed by a de-excitation to the final state in which the phonons are emitted.¹⁴ The U_{eff} values are comparable in magnitude for 3 and 4; the difference between them primarily arises from the zero-field fitting parameter since the spin values are equivalent for these compounds. In fact, it appears that the structural distortion around the metal center plays a key role in the overall magnetic anisotropy. Elevating the Co(II) center above the N_4 mean plane from 0.39 Å in complex 3 to 0.52 Å in 4 (Figure 3 insets) is a structural anisotropy that may lead to the difference in the magnetic anisotropy observed for these two compounds. Although the axial zero-field splitting parameter (D) was not obtained using reduced magnetization data, it is reasonable to estimate a negative D value

from the acquired barriers ($U = (S^2 - 1/4)|D|$). As such, D values of -8 K and -12 K can be obtained for **3** and **4**, respectively. These estimated values are lower than the values determined through the dc susceptibility fit (*vide supra*), and this may be due to the non-negligible QTM present in these molecules. In order to precisely quantify the axial (D) and rhombic (E) ZFS parameters, we are currently investigating single crystals of both samples using HF EPR methods.

Our goal, to design and synthesize a geometrically controlled Co(II) species, led to air-stable mononuclear Co(II) square pyramidal complexes where slow relaxation of the magnetization was achieved and enhanced through introduction of spin-orbit coupling. By employing the rigid, planar tridentate coordination environment from the bis(imino)pyridine pincer ligand in conjunction with two accommodating isothiocyanate ligands, it was possible to specify the orientation of the basal plane of this geometry. Through changes to the ligand substituents, distortions around the metal center were modulated to induce a structural distortion and promote elevation of the Co(II) ion which, in turn, leads to significant spin-orbit coupling. Both complexes exhibit SMM-like behavior under applied static dc fields with the more distorted complex **4** exhibiting the larger anisotropic barrier. Additionally, solution methods were employed in order to eliminate intermolecular interactions and to validate that the observed slow relaxation of the magnetization arises strictly from a molecular origin rather than from collective behavior. The presented study demonstrates that structural fine-tuning can be utilized to shed light on the intricate role of spin-orbit coupling in slow relaxation of the magnetization and inspires our further investigations in this field.

■ ASSOCIATED CONTENT

S **Supporting Information.** Crystallographic data (cif files) for **3** and **4**, experimental procedures, computational modeling, and additional magnetic data. Figures S3–S15. This material is available free of charge via the Internet at <http://pubs.acs.org>.

■ AUTHOR INFORMATION

Corresponding Authors

darrin@uottawa.ca

■ ACKNOWLEDGMENT

We thank NSERC, CFI, ERA for funding and Matthew Decan from the Scaiano group for help with UV-vis measurements.

■ REFERENCES

- (1) (a) Milios, C. J.; Vinslava, A.; Wernsdorfer, W.; Moggach, S.; Parsons, S.; Perlepes, S. P.; Christou, G.; Brechin, E. K. *J. Am. Chem. Soc.* **2007**, *129*, 2754. (b) Christou, G.; Gatteschi, D.; Hendrickson, D. N.; Sessoli, R. *MRS Bull.* **2000**, *25*, 66. (c) Thomas, L.; Lionti, L.; Ballou, R.; Gatteschi, D.; Sessoli, R.; Barbara, B. *Nature* **1996**, *383*, 145. (d) Sokol, J. J.; Hee, A. G.; Long, J. R. *J. Am. Chem. Soc.* **2002**, *124*, 7656. (e) Maheswaran, S.; Chastanet, G.; Teat, S. J.; Mallah, T.; Sessoli, R.; Wernsdorfer, W.; Winpenny, R. E. P. *Angew. Chem.* **2005**, *44*, 5044.
- (2) (a) Ishikawa, N.; Sugita, M.; Wernsdorfer, W. *J. Am. Chem. Soc.* **2005**, *127*, 3650. (b) Jiang, S.-D.; Wang, B.-W.; Sun, H.-L.; Wang, Z.-M.; Gao, S. *J. Am. Chem. Soc.* **2011**, *133*, 4730. (c) Li, D. P.; Wang, T. W.; Li, C. H.; Liu, D. S.; Li, Y. Z.; You, X. Z. *Chem. Commun.* **2010**, *46*, 2929. (d) AlDamen, M. A.; Clemente-Juan, J. M.; Coronado, E.; Marti-Gastaldo, C.; Gaita-Arino, A. *J. Am. Chem. Soc.* **2008**, *130*, 8874.

- (e) Rinehart, J. D.; Long, J. R. *J. Am. Chem. Soc.* **2009**, *131*, 12558. (f) Jiang, S. D.; Wang, B. W.; Su, G.; Wang, Z. M.; Gao, S. *Angew. Chem., Int. Ed.* **2010**, *49*, 7448. (g) Magnani, N.; Apostolidis, C.; Morgenstern, A.; Colineau, E.; Griveau, J.-C.; Bolvin, H.; Walter, O.; Caciuffo, R. *Angew. Chem.* **2011**, *50*, 1696. (i) Rinehart, J. D.; Meihaus, K. R.; Long, J. R. *J. Am. Chem. Soc.* **2010**, *132*, 7572.

- (3) (a) Harman, W. H.; Harris, T. D.; Freedman, D. E.; Fong, H.; Chang, A.; Rinehart, J. D.; Ozarowski, A.; Sougrati, M. T.; Grandjean, F.; Long, G. J.; Long, J. R.; Chang, C. J. *J. Am. Chem. Soc.* **2010**, *132*, 18115. (b) Freedman, D. E.; Harman, W. H.; Harris, T. D.; Long, G. J.; Chang, C. J.; Long, J. R. *J. Am. Chem. Soc.* **2010**, *132*, 1224.

- (4) A recent organometallic Fe(II) SMM is reported in Weismann, D.; Sun, Y.; Lan, Y.; Wolmershauser, G.; Powell, A. K.; Sitzmann, H. *Chem.—Eur. J.* **2011**, *17*, 4700.

- (5) (a) Small, B. L.; Brookhart, M. *J. Am. Chem. Soc.* **1998**, *120*, 7143.

- (b) Britovsek, G. J. P.; Gibson, V. C.; Kimberley, B. S.; Maddox, S. J.; Solan, G. A.; White, A. J. P.; Williams, D. J. *Chem. Commun.* **1998**, 849.

- (6) Bowman, A. C.; Milsman, C.; Hojilla Atienza, C. C.; Lobkovsky, E.; Wieghardt, K.; Chirik, P. J. *J. Am. Chem. Soc.* **2010**, *132*, 1676. Hojilla Atienza, C. C.; Bowman, A. C.; Lobkovsky, E.; Chirik, P. J. *J. Am. Chem. Soc.* **2010**, *132*, 16343.

- (7) (a) Jurca, T.; Korobkov, I.; Yap, G. P. A.; Gorelsky, S. I.; Richeson, D. S. *Inorg. Chem.* **2010**, *49*, 10635. (b) Jurca, T.; Dawson, K.; Mallov, I.; Burchell, T. J.; Yap, G. P. A.; Richeson, D. S. *Dalton Trans.* **2010**, *39*, 1266. (c) Jurca, T.; Lummis, J.; Burchell, T. J.; Gorlesky, S. I.; Richeson, D. S. *J. Am. Chem. Soc.* **2009**, *131*, 4608.

- (8) Cirera, J.; Ruiz, E.; Alvarez, S.; Neese, F.; Kortus, J. *Chem.—Eur. J.* **2009**, *15*, 4078.

- (9) Related bis(imino)pyridine Co(SCN)₂ complexes are reported in Sacconi, L.; Morassi, R.; Midollini, S. *J. Chem. Soc. A* **1968**, 1510.

- (10) Mabbs, F. E.; Machin, D. J. *Magnetism and Transition Metal Complexes*; Dover Publications: 2008.

- (11) Kooistra, T. M.; Hekking, K. F. W.; Knijnenburg, Q.; de Bruin, B.; Budzelaar, P. H. M.; de Gelder, R.; Smits, J. M. M.; Gal, A. W. *Eur. J. Inorg. Chem.* **2003**, 648.

- (12) A simple DFT model corroborating this proposition is provided in the Supporting Information.

- (13) Davidson, E. R. *MAGNET*; Indiana University: Bloomington, IN, 1999.

- (14) (a) Chirico, R. D.; Carlin, R. L. *Inorg. Chem.* **1980**, *19*, 3031. (b) Hung, S.-W.; Yang, F.-A.; Chen, J.-H.; Wang, S.-S.; Tung, J.-Y. *Inorg. Chem.* **2008**, *47*, 7202.

- (15) Luis, F.; Mettes, F.; Evangelisti, M.; Morello, A.; de Jongh, L. J. *J. Phys. Chem. Solids* **2004**, *65*, 763.

- (16) (a) Wernsdorfer, W.; Bhaduri, S.; Boskovic, C.; Christou, G.; Hendrickson, D. N. *Phys. Rev. B* **2002**, *65*, No. 180403. (b) Wernsdorfer, W.; Chakov, N. E.; Christou, G. *Phys. Rev. Lett.* **2005**, *95*, No. 037203.

- (17) Orbach, R. *Proc. R. Soc. London, Ser. A* **1961**, *264*, 458. (b) Orbach, R. *Proc. R. Soc. London, Ser. A* **1961**, *264*, 458.